Macromolecules

NOTE

pubs.acs.org/Macromolecules

Branching at High Frequency Pulsed Laser Polymerizations of Acrylate Monomers

Yuri Reyes,[†] Gurutze Arzamendi,[‡] José M. Asua,[†] and Jose R. Leiza*[,†]

[†]Institute for Polymer Materials, POLYMAT, and Kimika Aplikatuko Departamentua, Kimika Zientzien Fakultatea, University of the Basque Country (UPV/EHU), Joxe Mari Korta zentroa, Tolosa hiribidea 72, Donostia-San Sebastián 20018, Spain

[‡]Departamento de Química Aplicada, Universidad Pública de Navarra, Campus de Arrosadia, 31006 Iruña-Pamplona, Spain

Supporting Information

INTRODUCTION

Pulsed laser polymerization (PLP) coupled with size exclusion chromatography(SEC) has been adopted by the IUPAC as the method of choice to determine propagation rate constants of monomers in free-radical polymerization.[1−3] Benchmark values for some important monomers are available.[4−9] Recently, the use of PLP has been extended to the estimation of rate constants of other reaction mechanisms of free-radical polymerization such as propagation rate constants of tertiary radicals in acrylates[10] and termination rate coefficients.[11] In PLP experiments, the monomer (optionally solvent) and a photoinitiator are irradiated by a laser pulse. The radicals generated by this pulse will grow and eventually terminate resulting in a decreasing radical concentration. The concentration of radicals sharply increases with the subsequent pulse, and this leads to the sudden termination of a large fraction of radicals generated by the previous pulse. Still a fraction of the radicals produced in the first pulse survives until radicals generated in the subsequent pulses terminate them. Thus, the degree of polymerization of a polymer chain that grows over n laser pulses before being terminated is given by:

$$L_n = nk_p[M]t_d; \quad n = 1, 2, \ldots \tag{1}$$

where [M] is the concentration of monomer, t_d is the time between pulses, namely, the inverse of the laser pulse frequency, and k_p is the propagation rate constant. It is well accepted that L_1 is best identified with the first inflection point on the low molecular weight side of the MWD peak.[4−6] In practice, the inflection point is determined at the first maximum of the first derivative of the $W(\log M)$ vs $\log M$ curve.[12] In the PLP experiments, several consistency tests must be fulfilled in order to obtain reliable k_p values. The most important are as follows: (i) the occurrence of at least a secondary inflection point, L_2, located at twice the molecular weight of the first inflection point; (ii) the k_p value has to be independent of the radical concentration and pulsed frequency used in the experiments.

The consistency requirements are fulfilled as long as the initiation and termination of radicals are mostly controlled by the laser pulses; in other words as far as the time-chain length correlation given by eq 1 is maintained. If other reaction events occur between pulses distorting the time-chain length correlation, the accurate determination of k_p might not be possible. Thus, Arzamendi et al.[13] demonstrated by means of Monte Carlo simulations of PLP/SEC experiments that at low laser frequencies (up to 100 Hz) the difficulties encountered to obtain the propagation rate constants of n-butyl acrylate at temperatures above 30 °C[14−16] were due to the backbiting process that converted the secondary radicals to tertiary radicals. The tertiary radicals are much less reactive than the secondary ones and this leads to a distribution of the average propagation rate of each growing chain resulting in a featureless MWD, which cannot be used to determine k_p (in this work, k_p, refers to the propagation rate coefficient of secondary radicals). As the activation energy of the backbiting is higher than that of the propagation (see Table 2) the formation of the tertiary radicals is substantial at temperatures above 30 °C. Therefore, the PLP/SEC method was not consistent and k_p values could not be accurately measured. The level of branching predicted by the Monte Carlo simulations were in agreement with branching measured in poly(n-butyl acrylate) produced in PLP experiments carried out at 100 Hz at different temperatures and monomer concentrations.[17] Simulations showed that a branching density of 0.3% (3 branches per 1000 monomer molecules polymerized) was enough to produce a featureless MWD.[13] Recently, Barner-Kowollik et al.[18] showed that PLP/SEC experiments of n-BA carried out at 500 Hz allowed to obtain k_p values at temperatures well above 30 °C. The k_p data gathered in the range 10 to 70 °C at this frequency agreed very well with the data obtained by the working party of the IUPAC at lower frequencies in the range −65 and 20 °C.[8] The authors claimed that at this high frequency the occurrence of the backbiting process is considerably reduced, even at temperatures above 30 °C, and therefore well-defined MWD structures are obtained in the PLP/SEC experiments leading to an accurate determination of k_p. However, the authors did not report the branching level of the polymers produced in the PLP experiments carried out at high frequencies. In addition, no clear reason for the reduction of the backbiting was offered.

The aim of this work is 2-fold. First, to unveil the reasons for the reduction of the backbiting when pulse laser frequency is increased in PLP experiments. Second, to provide a map of the temperature-pulse frequency plot where the accurate determination of k_p is possible. The polymerization of n-butyl acrylate was used as case study.

Received: February 19, 2011
Revised: April 5, 2011
Published: April 14, 2011

Table 1. Average Characteristic Times of the Different Processes[a]

process	average characteristic time	t_d (s, at 40 °C)
propagation of secondary radicals	$t_1 = 1/(k_p[M])$	6.27×10^{-6}
propagation of tertiary radicals	$t_2 = 1/(k_p^*[M])$	6.25×10^{-3}
intramolecular chain transfer to polymer	$t_3 = 1/k_{bb}$	2.3×10^{-3}
intermolecular chain transfer to polymer	$t_4 = 1/(k_{tr}^{pol}[Pol])$	16.95/[Pol]
chain transfer of secondary radicals to monomer	$t_5 = 1/(k_{tr}^{mon}[M])$	0.11
chain transfer of tertiary radicals to monomer	$t_6 = 1/(k_{tr}^{*\,mon}[M])$	35
β-scission	$t_7 = 1/k_\beta$	31
propagation to pendant double bond	$t_8 = 1/(k_{mac}[TDB])$	8×10^{-5}/[TDB]
bimolecular termination of secondary radicals	$t_9 = 1/(kt_1[R_1])$	1.9×10^{-4} [b]
bimolecular termination of tertiary radicals	$t_{10} = 1/(kt_2[R_2])$	3.6×10^{-2} [b]
bimolecular cross-termination of secondary and tertiary radicals	$t_{11} = 1/(kt_{12}[R_i])$, $i = 1$ or 2	2.63×10^{-3} [b]

[a] [M] = 6.9 mol/L. [Pol] and [TDB] refer to polymer and terminal double bond concentrations. [b] For a reference value of $[R_1] = [R_2] = 1 \times 10^{-5}$ mol/L.

Table 2. Values of the Rate Coefficients Used in the Monte Carlo Simulations of the Polymerization of *n*-BA

parameter	Arrhenius pre-exponential factor	activation energy, kJ/mol	value at 40 °C	reference
k_p (L/mol s)	2.21×10^7	17.9	22 744	8
k_p^* (L/mol s)	1.52×10^6	28.9	22.8	10
k_{bb} (s^{-1})	1.81×10^7	27.7	433	20
k_{tr}^{pol} (L/mol s)	2.48×10^3	27.7	5.9×10^{-2}	21
k_{tr}^{mon} (L/mol s)	2.88×10^5	32.6	1.04	22
$k_{tr}^{*,mon}$ (L/mol s)	2.00×10^5	46.1	4.0×10^{-3}	22
k_β (s^{-1})	1.49×10^9	63.9	3.2×10^{-2}	23
k_{mac} (L/mol s)	$k_p \times 0.5$	-	12 509	19
k_{t1} (L/mol s)	1.3×10^{10}	8.4	5.15×10^8	11
k_{t2} (L/mol s)	1.29×10^7	4.0	2.8×10^6	20
k_{c12}(L/mol s)	$(k_{t1}k_{t2})^{0.5}$	-	3.79×10^7	11, 20

MONTE CARLO SIMULATIONS OF PLP EXPERIMENTS

The kinetic scheme considers initiation of radicals by a laser pulse, propagation of secondary radicals, formation of tertiary radicals by means of backbiting and intermolecular chain transfer to polymer of secondary radicals, propagation of tertiary radicals, chain transfer to monomer of both radicals, β-scission of tertiary radicals, propagation to chains containing terminal double bonds (formed by either β-scission and chain transfer to monomer), and termination by combination of both type of radicals.[13,19]

Each reaction event has an average characteristic time, which is given by the inverse of the rate of the process ($t_i = 1/R_{pi}$, Table 1).

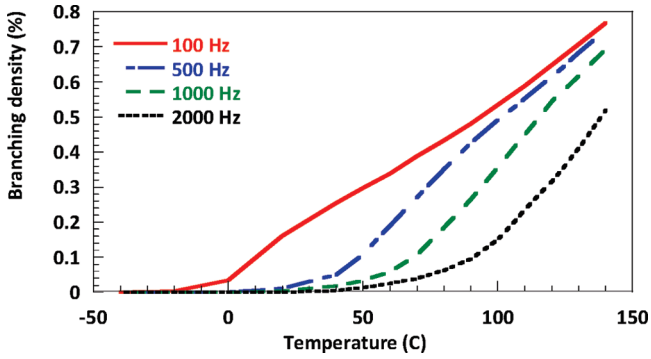

Figure 1. Simulated branching density as a function of temperature for PLP experiments of *n*-BA in bulk conditions at different frequencies.

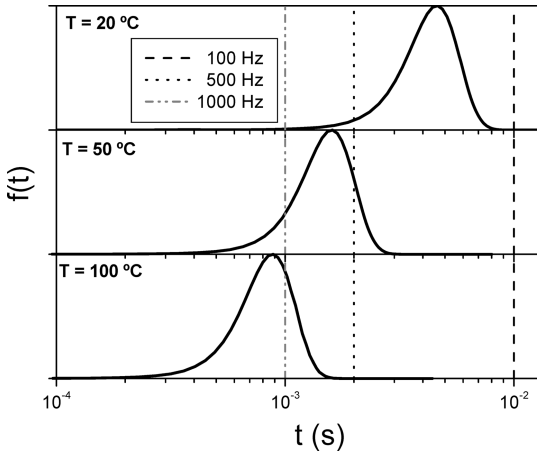

Figure 2. Comparison of the distribution of the characteristic times of the backbiting reaction mechanism at different temperatures and the laser pulsed frequencies. The vertical lines correspond to the time between pulses (inverse of the laser pulse frequencies in seconds).

The time actually spent in each individual reaction event is distributed around the average characteristic time of the process. It was assumed that, for all reaction events, they were distributed according to a Gaussian distribution of variance $\sigma^2 = 0.5$. On the other hand, in PLP experiments a huge number of radicals are generated at each pulse time and although most of the radicals generated in the previous pulse terminate some of them survive one or more pulses. The fraction of radicals that survive a pulse is given by $\alpha = 1/(1 + k_t[R]_0 t_d)$ where k_t is the termination rate coefficient, $[R]_0$ is the concentration of radicals at the beginning of the pulse and t_d is the inverse of the pulse frequency.[16] For PLP experiments of *n*-BA at low pulse frequencies (<200 Hz) the fraction of radicals that survive a pulse is small and hence t_d can be considered as the life expectancy of a growing radical. However, as the pulse frequency increases, α increases and hence the life expectancy of a substantial fraction of the growing radicals is higher than t_d.

In the Monte Carlo simulation, 10 000 radicals with a concentration of 1×10^{-5} mol/L were considered to be produced by each laser pulse. The events that each of these radicals undergo (analyzed sequentially) were selected based on the probability of the corresponding reaction mechanism, provided that the time needed to undergo the chosen reaction did not exceed the life expectancy of the radical. Specifically, for each chain that has

dx.doi.org/10.1021/ma200389h |*Macromolecules* 2011, 44, 3674–3679

been growing a time t_{gc}, the next reaction event was chosen by a unit-interval uniformly distributed random number, r_1, according to the following relation

$$\sum_{i=1}^{k-1} p_i < r_1 < \sum_{i=1}^{k} p_i \tag{2}$$

where P_i was the probability of reaction i given by

$$P_i = \frac{R_{pi}}{\sum_{i=1}^{R_e} R_{pi}}; \quad \sum_{i=1}^{R_e} P_i = 1 \tag{3}$$

where R_{pi} is the rate of the ith reaction and Re is the number of reactions that the radical can undergo.

The chosen reaction (k) was allowed to occur if

$$t_{gc} + t'_k \leq n_{ps} t_d \tag{4}$$

Otherwise, a new possible next event was chosen from eq 2. In eq 4, t_{gc} was the time that the chain has been growing, t'_k the time needed to undergo reaction k (obtained from the Gaussian distribution around the characteristic time of reaction k), t_d the time between pulses and n_{ps} is the number of pulses that a growing radical might survive. In other words, $n_{ps}t_d$ is the life expectancy of the growing radical. A random number, r_2, was used to determine n_{ps}. The value of n_{ps} was calculated as follows:

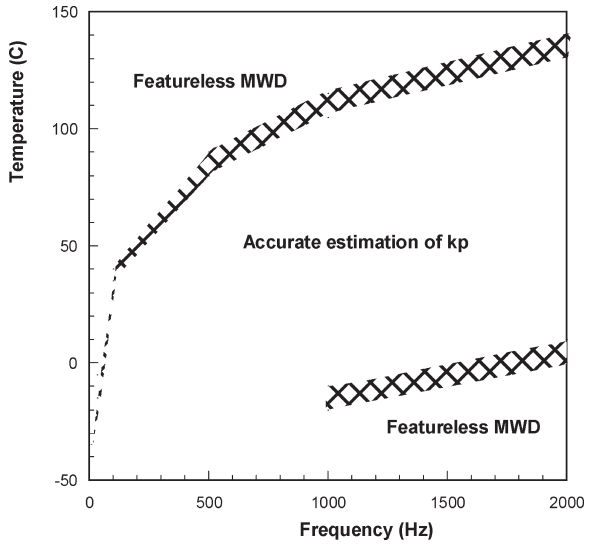

Figure 3. Temperature−pulse frequency map for accurate determination of the k_p for *n*-BA.

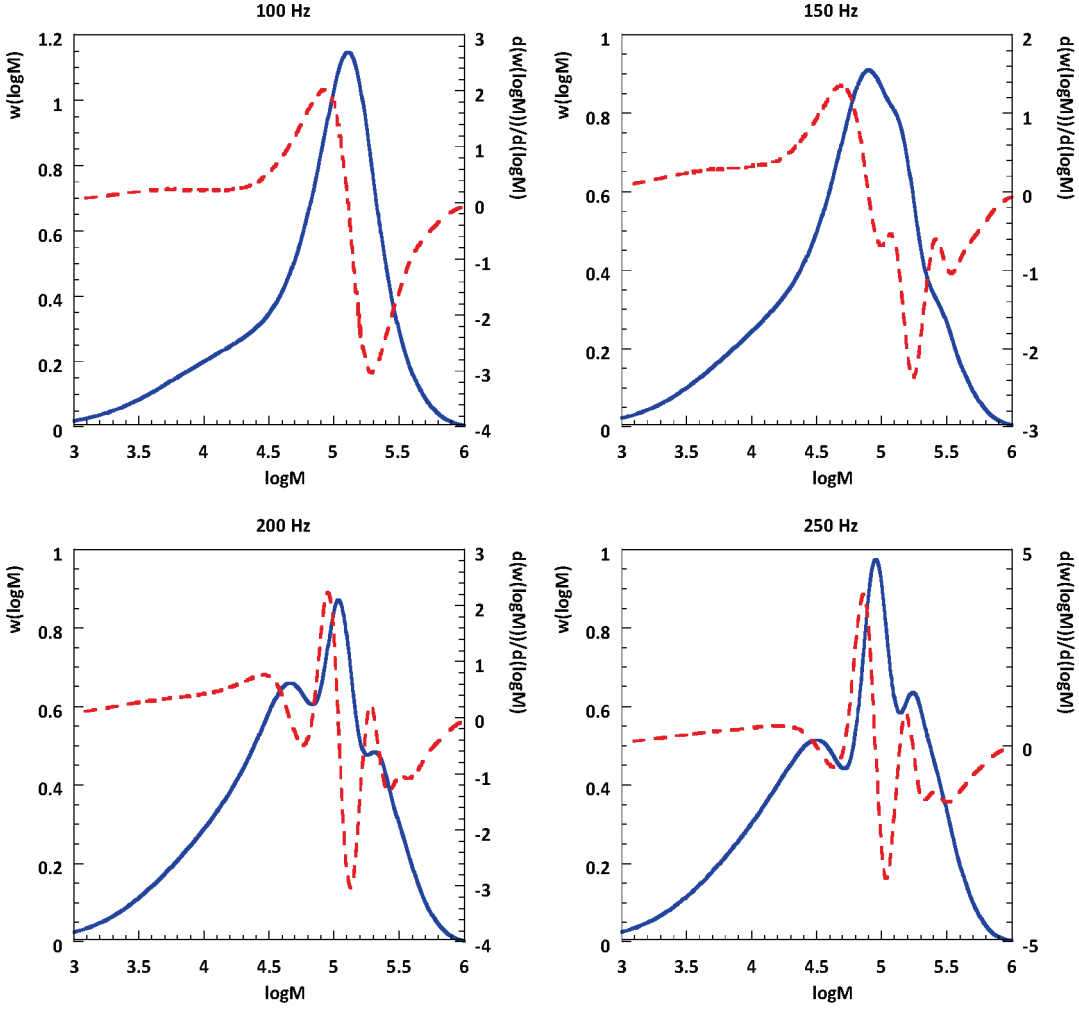

Figure 4. Simulated MWD (solid line) and derivative (dashed) generated in PLP experiments of *n*-BA carried out in bulk conditions at 40 °C. (a) 100 Hz; (b) 150 Hz; (c) 200 Hz; (d) 250 Hz.

dx.doi.org/10.1021/ma200389h |*Macromolecules* 2011, 44, 3674–3679

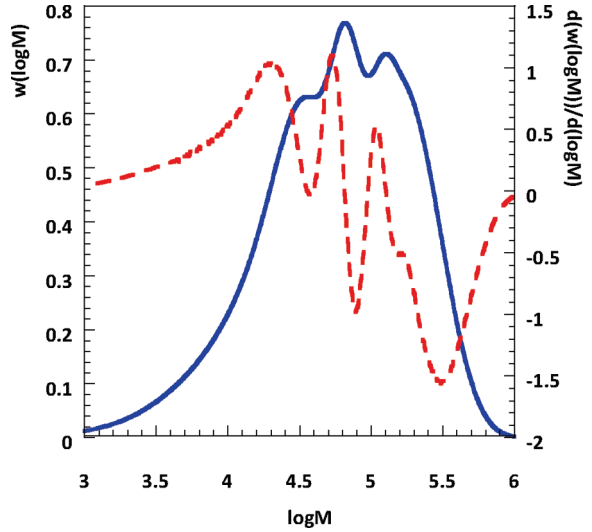

Figure 5. Simulated MWD (solid line) and derivative (dashed) generated in the PLP experiments of *n*-BA carried out in bulk conditions at 100 °C and 1000 Hz.

if r_2 is between 1 and $1 - \alpha$, $n_{ps} = 1$; if r_2 is between $1 - \alpha$ and $1 - \alpha^2$, $n_{ps} = 2$; if r_2 is between $1 - \alpha^2$, and $1 - \alpha^3$, $n_{ps} = 3$ and so on.

The values of the kinetic parameters used in the simulations are given in Table 2

RESULTS

PLP experiments for *n*-BA under bulk conditions were simulated at temperatures from −40 to 140 °C at laser pulse frequencies in the range 10−2000 Hz. Figure 1 presents the effect of the temperature and pulse frequency (only four pulse frequencies are shown for clarity) on the branching density (number of tertiary radicals that propagated or terminated divided by the total number of polymerized monomer units). Figure 1 plots the branching density in percentage.

It can be seen that branching density increased with temperature, and for a given temperature, the increase in laser pulse frequency considerably reduced the branching density. For instance, at 40 °C and 100 Hz, branching density was ca. 0.3% (3 branches per 1000 monomer molecules) whereas at 500 Hz, the branching density was well below 0.1%, and the branching density was negligible at higher frequencies. The simulation model clarified the reasons for the decrease of branching density as the pulse frequency increased. Under the conditions used for the PLP of acrylates, branching mainly results from the intramolecular chain transfer to polymer (followed by propagation of the resulting tertiary radical). Figure 2 compares the distribution of the characteristic time for the backbiting process at 20, 50, and 100 °C with the time between laser pulses at 100, 500, and 1000 Hz indicated by the vertical lines in the plot. It can be seen that at 20 °C the characteristic times for backbiting were shorter than the time between laser pulses at 100 Hz, and hence backbiting could occur. On the other hand, the characteristic times for backbiting were longer than the time between laser pulses at 500 and 1000 Hz, and therefore backbiting was less probable (for instance, it led to a negligible branching at 500 Hz) or virtually impossible at 1000 and above. As temperature increases, the characteristic times for backbiting decrease, and hence backbiting could occur at higher pulse frequencies, but in any case, the likelihood of occurrence of backbiting decreased with the pulse frequency. Consequently, the reason for the decrease of branching density with pulse frequency was that the time between laser pulses became shorter than the characteristic time for the backbiting.

The increase of branching density with temperature for a given pulse frequency was due to two reasons. First, because the characteristic time for backbiting decreased reducing the effect of the time between laser pulses on the occurrence of backbiting. Second, the activation energy for backbiting is higher than that of the propagation.

A consequence of the occurrence of substantial backbiting is that the molecular weight distribution is broadened by the stochastic switch between secondary and tertiary radicals (for a given growing time, chains that suffer backbiting are shorter than those that do not). This leads to a featureless molecular weight distribution, which cannot be used to accurately estimate k_p. An extensive simulation study was carried out aiming to determine the temperature-pulse frequency map where accurate determination of k_p for BA can be obtained (see Supporting Information). Figure 3 presents this map. The map shows three regions separated by thick border lines. Accurate estimation of k_p can be achieved in the center region. The criterion used to draw the upper border (gray areas) was the minimum pulse frequency needed to obtain a significant MWD at a given temperature (or for a given laser pulse frequency, the maximum temperature at which the MWD changes from a PLP structure to a featureless MWD).

Figure 4 illustrates this transition at 40 °C. This plot presents the MWD together with the derivative of the w(log M) used to compute k_p. It can be seen that a featureless MWD was obtained at 100 Hz, whereas a well-defined MWD was obtained for pulse frequencies greater than 200 Hz. The reason for the featureless MWD obtained at low frequencies was the occurrence of backbiting. Higher frequencies reduce the backbiting and hence allow the k_p to be accurately estimated at higher temperatures.

The area at the bottom of Figure 3 also separates a region were PLP structure cannot be obtained. In this region (very low temperatures and high frequencies), the reason for the featureless MWD was not backbiting, but the very short lifetime of the chains (due to the high frequencies) and the low termination rate of the chains that reduced the termination of radicals during the pulse required to obtain a significant MWD.[16] In order to escape from this low termination region, one needs to reduce the frequency, which will increase the likelihood of backbiting, and hence limit the maximum temperature attainable. As shown in the temperature-pulse frequency map at frequencies lower than 1000 Hz the low termination region does not create featureless MWD and hence k_p can be obtained at low temperatures. Therefore, experiments should be carried out at least at two frequencies if the kp value in a broad temperature range (−40/140 °C) is required.

As discussed in the Supporting Information, the thickness of the frontiers between the different areas are affected by the standard deviation used in the Gaussian distribution that was applied to each chain length in order to mimic instrumental broadening of the SEC measurements. Nevertheless, the usefulness of the map is not significantly affected, and it may be used to guide future experimental work.

Thus, Figure 3 shows that accurate estimation of k_p can be obtained at 100 °C using a pulse frequency of 1000 Hz (the corresponding MWD and derivative of $w(\log M)$ are presented

in Figure 5). It is interesting to pointing out that in the region useful for accurate estimation of k_p, the branching level was lower than 0.3%.

The methodology presented in this work can be used to build maps of the PLP feasibility regions for any monomer. As the accuracy of the map increases with the accuracy of the rate coefficients, an iterative process can be envisaged. Preliminary maps based on uncertain rate coefficients are used to guide the first experiments that are used to improve the accuracy of the coefficients, which in turn lead to better and more accurate maps.

CONCLUSIONS

The branching density of poly(butyl acrylate) produced by pulse laser polymerization at a given temperature decreases by increasing the pulse frequency of the laser source because the characteristic time of backbiting (which is the main mechanism leading to the formation of branches) becomes larger than the time between laser pulses. The feasibility region in the temperature-pulse frequency map in which k_p can be accurately estimated has been identified. This map may be used to guide experimental work aiming at estimating the k_p at higher temperatures. An interesting finding is that in the feasibility region, the branching level was lower than 0.3%. This work was carried out with *n*-butyl acrylate but the methodology can be used to build maps for other monomers.

ASSOCIATED CONTENT

Supporting Information. PLP simulations of *n*-BA under bulk conditions. This material is available free of charge via the Internet at http://pubs.acs.org.

AUTHOR INFORMATION

Corresponding Author
*E-mail: jrleiza@ehu.es.

ACKNOWLEDGMENT

The financial support by the Basque Government (IT-303-07) and Ministerio de Educación y Ciencia (CTQ2006-03412/PPQ and Programa Consolider INgenio 2010 "CIC Nanogune Consolider" contract CSD 2006-00053) are greatly appreciated.

REFERENCES

(1) Beuermann, S.; Buback, M. Rate coefficients of free-radical polymerization deduced from pulsed laser experiments. *Prog. Polym. Sci.* **2002**, *27*, 191–254.

(2) Coote, M. L.; Zammit, M. D.; Davis, T. P. Determination of free-radical rate coefficients using pulsed-laser polymerization. *Trends Polym. Sci.* **1996**, *4*, 189–196.

(3) van Herk, A. M. Pulsed initiation polymerization applied to acrylate monomers: Sources of experimental failure. *Macromol. Rapid Commun.* **2001**, *22*, 687–689.

(4) Buback, M.; Gilbert, R. G.; Hutchinson, R. A.; Klumperman, B.; Kuchta, F. D.; Manders, B. G.; Odriscoll, K. F.; Russell, G. T.; Schweer, J. Critically Evaluated Rate Coefficients for Free-Radical Polymerization 0.1. Propagation Rate Coefficient for Styrene. *Macromol. Chem. Phys.* **1995**, *196*, 3267–3280.

(5) Beuermann, S.; Buback, M.; Davis, T. P.; Gilbert, R. G.; Hutchinson, R. A.; Olaj, O. F.; Russell, G. T.; Schweer, J.; vanHerk, A. M. Critically evaluated rate coefficients for free-radical polymerization 0.2. Propagation rate coefficients for methyl methacrylate. *Macromol. Chem. Phys.* **1997**, *198*, 1545–1560.

(6) Beuermann, S.; Buback, M.; Davis, T. P.; Gilbert, R. G.; Hutchinson, R. A.; Kajiwara, A.; Klumperman, B.; Russell, G. T. Critically evaluated rate coefficients for free-radical polymerization, 3 - Propagation rate coefficients for alkyl methacrylates. *Macromol. Chem. Phys.* **2000**, *201*, 1355–1364.

(7) Beuermann, S.; Buback, M.; Davis, T. P.; Garcia, N.; Gilbert, R. G.; Hutchinson, R. A.; Kajiwara, A.; Kamachi, M.; Lacik, I.; Russell, G. T. Critically evaluated rate coefficients for free-radical polymerization, 4 - Propagation rate coefficients for methacrylates with cyclic ester groups. *Macromol. Chem. Phys.* **2003**, *204*, 1338–1350.

(8) Asua, J. M.; Beuermann, S.; Buback, M.; Castignolles, P.; Charleux, B.; Gilbert, R. G.; Hutchinson, R. A.; Leiza, J. R.; Nikitin, A. N.; Vairon, J. P.; van Herk, A. M. Critically evaluated rate coefficients for free-radical polymerization, 5 - Propagation rate coefficient for butyl acrylate. *Macromol. Chem. Phys.* **2004**, *205*, 2151–2160.

(9) Beuermann, S.; Buback, M.; Hesse, P.; Kuchta, F. D.; Lacik, I.; van Herk, A. M. Critically evaluated rate coefficients for free-radical polymerization. Part 6: Propagation rate coefficient of methacrylic acid in aqueous solution. *Pure Appl. Chem.* **2007**, *79*, 1463–1469.

(10) Nikitin, A. N.; Hutchinson, R. A.; Buback, M.; Hesse, P. Determination of intramolecular chain transfer and midchain radical propagation rate coefficients for butyl acrylate by pulsed laser polymerization. *Macromolecules* **2007**, *40*, 8631–8641.

(11) Barth, J.; Buback, M.; Hesse, P.; Sergeeva, T. Termination and Transfer Kinetics of Butyl Acrylate Radical Polymerization Studied via SP-PLP-EPR. *Macromolecules* **2010**, *43*, 4023–4031.

(12) Olaj, O. F.; Bitai, I.; Hinkelmann, F. The Laser-Flash-Initiated Polymerization As A Tool of Evaluating (Individual) Kinetic Constants of Free-Radical Polymerization 0.2. the Direct Determination of the Rate-Constant of Chain Propagation. *Makromol. Chem.—Macromol. Chem. Phys.* **1987**, *188*, 1689–1702.

(13) Arzamendi, G.; Plessis, C.; Leiza, J. R.; Asua, J. M. Effect of the intramolecular chain transfer to polymer on PLP/SEC experiments of alkyl acrylates. *Macromol. Theory. Simul.* **2003**, *12*, 315–324.

(14) Couvreur, L.; Piteau, G.; Castignolles, P.; Tonge, M.; Coutin, B.; Charleux, B.; Vairon, J. P. Pulsed-laser radical polymerization and propagation kinetic parameters of some alkyl acrylates. *Macromol. Symp.* **2001**, *174*, 197–207.

(15) Lyons, R. A.; Hutovic, J.; Piton, M. C.; Christie, D. I.; Clay, P. A.; Manders, B. G.; Kable, S. H.; Gilbert, R. G. Pulsed-laser polymerization measurements of the propagation rate coefficient for butyl acrylate. *Macromolecules* **1996**, *29*, 1918–1927.

(16) Beuermann, S.; Paquet, D. A.; Mcminn, J. H.; Hutchinson, R. A. Determination of free-radical propagation rate coefficients of butyl, 2-ethylhexyl, and dodecyl acrylates by pulsed-laser polymerization. *Macromolecules* **1996**, *29*, 4206–4215.

(17) Plessis, C.; Arzamendi, G.; Alberdi, J. M.; van Herk, A. M.; Leiza, J. R.; Asua, J. M. Evidence of branching in poly(butyl acrylate) produced in pulsed-laser polymerization experiments. *Macromol. Rapid Commun.* **2003**, *24*, 173–177.

(18) Barner-Kowollik, C.; Gunzler, F.; Junkers, T. Pushing the Limit: Pulsed Laser Polymerization of *n*-Butyl Acrylate at 500 Hz. *Macromolecules* **2008**, *41*, 8971–8973.

(19) Wang, W.; Nikitin, A. N.; Hutchinson, R. A. Consideration of Macromonomer Reactions in *n*-Butyl Acrylate Free Radical Polymerization. *Macromol. Rapid Commun.* **2009**, *30*, 2022–2027.

(20) Arzamendi, G.; Leiza, J. R. Molecular weight distribution (soluble and insoluble fraction) in emulsion polymerization of acrylate monomers by Monte Carlo simulations. *Ind. Eng. Chem. Res.* **2008**, *47*, 5934–5947.

(21) Plessis, C.; Arzamendi, G.; Leiza, J. R.; Schoonbrood, H. A. S.; Charmot, D.; Asua, J. M. Modeling of seeded semibatch emulsion polymerization of *n*-BA. *Ind. Eng. Chem. Res.* **2001**, *40*, 3883–3894.

(22) Maeder, S.; Gilbert, R. G. Measurement of transfer constant for butyl acrylate free-radical polymerization. *Macromolecules* **1998**, *31*, 4410–4418.

(23) Nikitin, A. N.; Hutchinson, R. A.; Wang, W.; Kalfas, G. A.; Richards, J. R.; Bruni, C. Effect of Intramolecular Transfer to Polymer on Stationary Free-Radical Polymerization of Alkyl Acrylates, 5—Consideration of Solution Polymerization up to High Temperatures. *Macromol. React. Eng.* **2010**, *4*, 691–706.